ISME

A General Form Solution for Elastic Buckling of Thin Cylinders Made of FGM under Axial Loading

R. Shahsiah[*]
Assistant Professor

In this article, the axisymmetric mechanical buckling of thin cylindrical shell made of functionally graded material (FGM) is considered. The governing equations for a thin cylinder based on the first-order shell theory and Timoshenko's assumptions are obtained. The equations are derived using the Sanders simplified kinematic relations and the principle of work and energy. The constituent material of the functionally graded shell is assumed to be a mixture of ceramic and metal. It is assumed that the mechanical properties vary continuously through the shell thickness. The thin cylindrical shell is under uniform axial compressive load. The expression for the critical mechanical buckling load is obtained analytically and is given by closed form solution. The results are validated with the Timoshenko's formula in the literature.

Keywords: Axisymmetric; Buckling; Critical mechanical buckling load; Functionally graded material; Thin cylindrical shell

1 Introduction

In recent years, functionally graded materials (FGMs) have gained considerable importance in design of structures under high temperature environments. FGMs are also considered as potential structural materials whereas they were originally designed as thermal barriers for different engineering applications.

A survey of literature reveals that the problems of mechanical deformations and stresses in functionally graded cylindrical shells under mechanical loads have not been treated in a general form in the literature. Thermal buckling analysis of perfect cylindrical shells of isotropic and homogeneous materials and cylindrical shells of composite materials based on the Donnell and improved Donnell stability equations are studied by Eslami et al. [1-2]. Eslami and Shariyat considered the flexural theory and with the full Green nonlinear strain-displacement relation, instead of the simplified Sanders assumptions, formulated the dynamic mechanical and the thermal buckling of imperfect cylindrical shells [3]. The higher order shear deformation theory, including the normal stress, was used and the mixed formulation was established to simplify the approach of both kinematical and forced boundary conditions. The technique was then improved by the same authors to an exact three dimensional analysis of circular cylindrical shells based on the equations of motion and the full nonlinear Green

[*]Assistant Professor, Mech. Eng. Dep., I. A. U., Central Tehran Branch, Tehran, Iran, r.shahsiah@gmail.com

strain-displacement relations [4]. The Donnell and improved Donnell stability equations are employed to derive a closed form solution for the elastoplastic and creep buckling of cylindrical shells under mechanical loads at an elevated temperature [5]. Eslami and Shahsiah determined the critical thermal buckling loads for imperfect cylindrical shells [6]. They used the Donnell and the improved Donnell stability equations and two models for imperfection, namely; the Wan-Donnell and Koiter models. Many post buckling studies based on the classical shell theory of composite laminated thin cylindrical shells subjected to mechanical or thermal loading or their combinations are available in the literature, such as Birman and Bert [7] and Shen [8-10]. Relatively few studies involving the application of shear deformation shell theory to post buckling analysis can be found in the literature, such as those given by Iu and Chia [11] and Reddy and Savoia [12]. In these studies, the material properties are considered to be independent of temperature.

Studies of temperature and moisture effects on the buckling loads of laminated flat and cylindrical panels are limited in number (Whitney and Ashton [13], Snead and Palazotto [14], Lee and Yen [15], Ram and Sinha [16], and Chao and Shyu [17]), where all these studies assumed perfectly initial configuration. Palazotto et al. [18-29] have done extensive theoretical and experimental work on the stability of composite panels. Their work substantially reduced the gap between the theoretical and experimental works. Shen [30] gave a full nonlinear post buckling analysis of composite laminated cylindrical shells subjected to combined loading of axial compression and external pressure under hygrothermal conditions.

Buckling analysis of structures made of FGM is recently reported in the literature. Birman [31] studied the buckling problem of functionally graded composite rectangular plate subjected to the uniaxial compression. The stabilization of a functionally graded cylindrical shell under axial harmonic loading is investigated by Ng et al. [32]. Shahsiah and Eslami presented the thermal buckling of cylindrical and spherical shells made of functionally graded material based on the first order shell theory and the Donnell and improved Donnell equations [33-35]. The buckling analysis of circular plates made of FGM is given by Najafizadeh and Eslami [36]. Javaheri and Eslami presented the thermal and mechanical buckling of rectangular plates made of FGM based on the first and higher order plate theories [37-40].

In this article, the axisymmetrical buckling load of functionally graded thin cylindrical shell is derived. The cylindrical shell is under uniform axial compressive load. The expression for the critical mechanical buckling load is obtained analytically and is given by closed form solution. In principal, the equations are derived using the Sanders simplified kinematic relations and the principle of work and energy.

2 Derivations

If a cylindrical shell is uniformly compressed in the axial direction, symmetrical buckling with respect to the axis of cylinder may occur at a certain value of the compressive load. As long as the shell remains cylindrical, the total strain energy is the strain energy due to axial compression. However, when buckling begins, in addition to the axial compression, the strain of the middle surface in the circumferential direction and also bending of the shell must also be considered. At the critical value of load, the increase in strain energy must be equal to the work done by the compressive load as the cylinder shortens owing to buckling (derived from the principle of work and energy).

Consider a functionally graded thin cylindrical shell of mean radius R, thickness h, and length L (Fig. 1). In the cylindrical shell x, θ, and z are the axial, circumferential, and radial directions, respectively (Fig. 2).

For simply supported boundary conditions, lateral displacements are given as

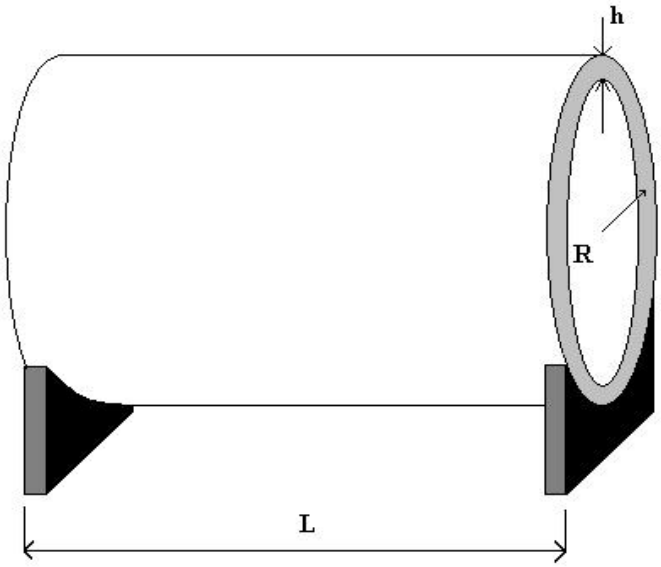

Figure 1 The Geometry of Cylindrical Shell with Simply Supported Edge Conditions (mean radius R, thickness h, and length L)

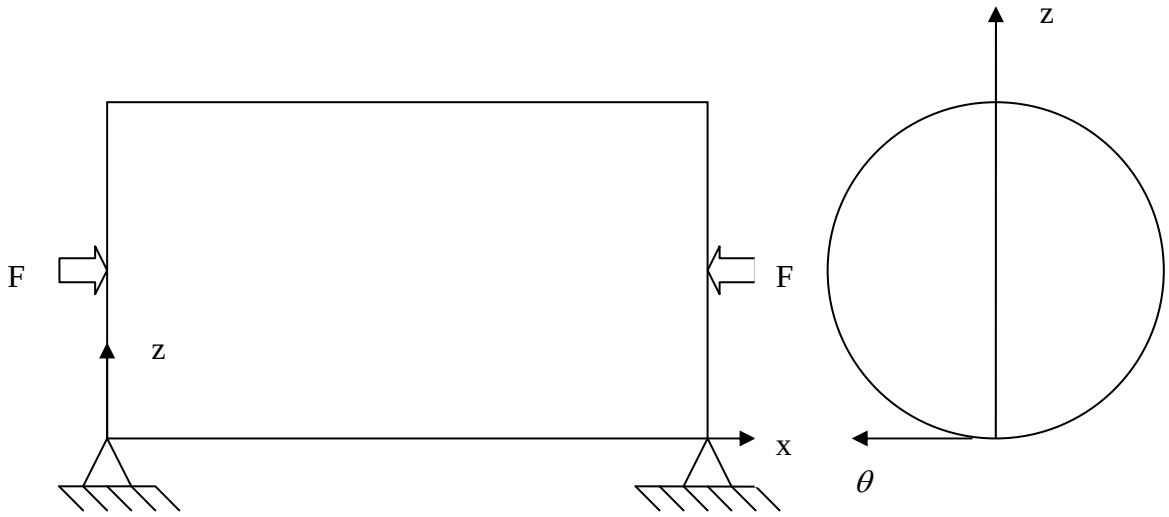

Figure 2 The Cylindrical Shell under Compressive Load F. In the Cylindrical Shell x, θ, and z are the Axial, Circumferential, and Radial Directions, Respectively.

$$w = -A\sin\frac{m\pi x}{L} \tag{1}$$

where m is the number of longitudinal buckling waves (buckling modes). The middle surface normal strains are ε_{xm} and $\varepsilon_{\theta m}$ in the axial and circumferential directions, respectively. After buckling, these strains are deduced from the condition that the axial compressive force during buckling remains constant (Timoshenko's assumption). The axial strain before buckling is given as

$$\varepsilon_0 = -\frac{N_{cr}}{E(z)h} \tag{2}$$

where $E(z)$ and N_{cr} are the elastic modulus and the critical buckling load, respectively. After buckling, the axial strain is obtained as

$$\varepsilon_{xm} + \nu\varepsilon_{\theta m} = (1-\nu^2)\varepsilon_0 = -(1-\nu^2)\frac{N_{cr}}{E(z)h} \tag{3}$$

where ν is Poisson's ratio and in this article it is considered to be a constant and not a function of the radial direction z.
Observing that

$$\varepsilon_{\theta m} = -\nu\varepsilon_0 - \frac{w}{R} = \frac{\nu N_{cr}}{E(z)h} + \frac{A}{R}\sin\frac{m\pi x}{L} \tag{4}$$

$$\varepsilon_{xm} = \varepsilon_0 + \nu\frac{w}{R} = -\frac{N_{cr}}{E(z)h} - \nu\frac{A}{R}\sin\frac{m\pi x}{L} \tag{5}$$

the change of curvature in the axial and circumferential directions are given as [41]

$$k_x = w_{,xx} \tag{6}$$

$$k_\theta = \frac{1}{R^2}\left(\frac{\partial v}{\partial\theta} + \frac{\partial^2 w}{\partial\theta^2}\right) \tag{7}$$

$$k_{x\theta} = \frac{1}{R}\left(\frac{\partial v}{\partial x} + \frac{\partial^2 w}{\partial x\partial\theta}\right) \tag{8}$$

where the notation ∂ indicates a partial derivative and v is circumferential displacement. The strain energy of a deformed shell consists of two parts: (1) the strain energy due to the bending and (2) the strain energy due to the stretching of the middle surface. For the isotropic shell, the bending strain energy is given as [41]

$$U_b = \frac{D}{2}\iint_A [k_x{}^2 + k_\theta{}^2 + 2\nu k_x k_\theta + 2(1-\nu)k_{x\theta}{}^2]dA \tag{9}$$

where D is the bending stiffness. For the isotropic shell, that part of the energy due to the stretching of the middle surface is as [41]

$$U_s = \frac{1}{2}\iint_A (N_x\varepsilon_{xm} + N_\theta\varepsilon_{\theta m} + N_{x\theta}\varepsilon_{x\theta m})dA \tag{10}$$

where N_{ij} and $\varepsilon_{x\theta m}$ are the resultant forces and shear strain of the middle surface, respectively. The resultant forces and moments per unit length expressed in terms of the stress components through the thickness, according to the first – order shell theory, are [41]

$$N_{ij} = \int_{-h/2}^{h/2} \sigma_{ij} dz \tag{11}$$

$$M_{ij} = \int_{-h/2}^{h/2} \sigma_{ij} z dz \tag{12}$$

where σ_{ij} are normal and shear stresses. For $i \neq j$, σ is replaced by τ. Consider Hook's law for a functionally graded thin cylindrical shell defined as [34]

$$\sigma_x = \frac{E(z)}{1-\nu^2}(\varepsilon_x + \nu\varepsilon_\theta) \tag{13}$$

$$\sigma_\theta = \frac{E(z)}{1-\nu^2}(\varepsilon_\theta + \nu\varepsilon_x) \tag{14}$$

$$\tau_{x\theta} = G(z)\varepsilon_{x\theta} \tag{15}$$

where $G(z)$ is shear modulus. The normal and shear strains at distance z from the shell middle surface are [41]

$$\varepsilon_x = \varepsilon_{xm} - zk_x \tag{16}$$

$$\varepsilon_\theta = \varepsilon_{\theta m} - zk_\theta \tag{17}$$

$$\varepsilon_{x\theta} = \varepsilon_{x\theta m} - 2zk_{x\theta} \tag{18}$$

Substituting Eqs. (16), (17), and (18) into Eqs. (13), (14), and (15) result in the constitutive equations in terms of the middle surface strains and curvatures as [34]

$$\sigma_x = \frac{E(z)}{1-\nu^2}[\varepsilon_{xm} + \nu\varepsilon_{\theta m} - z(k_x + \nu k_\theta)] \tag{19}$$

$$\sigma_\theta = \frac{E(z)}{1-\nu^2}[\varepsilon_{\theta m} + \nu\varepsilon_{xm} - z(k_\theta + \nu k_x)] \tag{20}$$

$$\tau_{x\theta} = G(z)[\varepsilon_{x\theta m} - 2zk_{x\theta}] \tag{21}$$

Substituting Eqs. (19), (20), and (21) into Eqs. (11) and (12) result in the forces and moments per unit length in terms of the middle surface strains and curvatures as [34]

$$N_x = \frac{C_1}{1-\nu^2}(\varepsilon_{xm} + \nu\varepsilon_{\theta m}) - \frac{C_3}{1-\nu^2}(k_x + \nu k_\theta) \tag{22}$$

$$N_\theta = \frac{C_1}{1-\nu^2}(\varepsilon_{\theta m} + \nu\varepsilon_{xm}) - \frac{C_3}{1-\nu^2}(k_\theta + \nu k_x) \tag{23}$$

$$N_{x\theta} = C_2\varepsilon_{x\theta m} - C_4 k_{x\theta} \tag{24}$$

$$M_x = \frac{C_3}{1-\nu^2}(\varepsilon_{xm} + \nu\varepsilon_{\theta m}) - \frac{C_5}{1-\nu^2}(k_x + \nu k_\theta) \tag{25}$$

$$M_\theta = \frac{C_3}{1-\nu^2}(\varepsilon_{\theta m} + \nu\varepsilon_{xm}) - \frac{C_5}{1-\nu^2}(k_\theta + \nu k_x) \tag{26}$$

$$M_{x\theta} = C_4\varepsilon_{x\theta m} - C_6 k_{x\theta} \tag{27}$$

The Coefficients $C_1, \ldots, C_6$ are the FGM constants and are given in Appendix (1).
The total potential energy of a thin cylindrical shell under axial compression is obtained by the sum of the bending and stretching strain energies and is given as [40]

$$U = U_b + U_s = \frac{1}{2}\iiint_{\forall} \frac{E(z)}{1-\nu^2}(\varepsilon_x{}^2 + \varepsilon_\theta{}^2 + 2\nu\varepsilon_x\varepsilon_\theta + \frac{1-\nu}{2}\varepsilon_{x\theta}{}^2)d\forall \tag{28}$$

Substituting Eqs. (16), (17), and (18) into Eq. (28) result in the total potential energy in terms of the middle surface strains and curvatures and is given in Appendix (2).
For the functionally graded thin cylindrical shell, observing that

$$U_b = \frac{C_5}{2(1-\nu^2)}\int_A [k_x{}^2 + k_\theta{}^2 + 2\nu k_x k_\theta + 2(1-\nu)k_{x\theta}{}^2]dA \tag{29}$$

$$U_s = \frac{1}{2}\int_A [N_x\varepsilon_{xm} + N_\theta\varepsilon_{\theta m} + N_{x\theta}\varepsilon_{x\theta m} - \frac{C_3}{1-\nu^2}\{\varepsilon_{xm}(k_x + \nu k_\theta) + \varepsilon_{\theta m}(k_\theta + \nu k_x)\}]dA \tag{30}$$

the function of the total potential energy in terms of the displacement components is obtained by substituting Eqs. (4), (5), (6), (7), (8), (22), (23), (24), (25), (26), and (27) into the total potential energy function and is given in Appendix (3). The expression for the increase of the total potential energy during buckling is given in Appendix (4). Assumptions of the symmetry of deformation are $\varepsilon_{x\theta m} = k_\theta = k_{x\theta} = 0$ or $u = u(x)$, $v = 0$, and $w = w(x)$. Considering a change of variable $y = R\theta$, the following expression is found for the increase of the total potential energy during buckling

$$\Delta U = \int_x\int_y [\frac{C_5 w,_{xx}\Delta w,_{xx}}{1-\nu^2} + \frac{C_1\varepsilon_0\Delta\varepsilon_0}{1-\nu^2} + \frac{C_1\nu\varepsilon_0\Delta w + C_1\nu w\Delta\varepsilon_0}{R(1-\nu^2)} - \frac{C_1\nu^3 w\Delta\varepsilon_0 + C_1\nu^3\varepsilon_0\Delta w}{R(1-\nu^2)}$$
$$- \frac{C_3 w,_{xx}\Delta\varepsilon_0 + C_3\varepsilon_0\Delta w,_{xx}}{2(1-\nu^2)} + \frac{C_1 w\Delta w}{R^2(1-\nu^2)} - \frac{C_1\nu^2\varepsilon_0\Delta\varepsilon_0}{1-\nu^2} - \frac{C_1\nu^2 w\Delta w}{R^2(1-\nu^2)} + \frac{C_3\nu^2 w,_{xx}\Delta\varepsilon_0}{2(1-\nu^2)}$$
$$+ \frac{C_3\nu^2\varepsilon_0\Delta w,_{xx}}{2(1-\nu^2)}]dxdy \tag{31}$$

In this equation, the symbol $\Delta(\ )$ refers to the state of stability and w is prebuckling lateral displacement. The longitudinal buckling mode shape Δw is defined by the same mode of prebuckling lateral displacement w as defined by (1) [41]. In the method that is applied by Timoshenko, during buckling, compressive load remain constant, and therefore $\Delta\varepsilon_0 = \varepsilon_0$. Substituting Eq. (1) in Eq. (31), gives

$$\Delta U = \frac{C_5 A^2 m^4 \pi^5 R}{L^3(1-\nu^2)} + \frac{2C_1\pi RLN_{cr}{}^2}{h^2 E(z)^2} + \frac{4C_1\nu N_{cr}AL}{hmE(z)}\{(-1)^m - 1\} + \frac{C_1 A^2\pi L}{R} +$$
$$\frac{2m\pi^2 RC_3 AN_{cr}}{LhE(z)}\{(-1)^m - 1\} \tag{32}$$

The work done by compressive forces during buckling is as

$$W = \frac{1}{2}\int_x\int_y \{N_x(\frac{\partial w}{\partial x})^2 + (\varepsilon_0 - \varepsilon_{xm})N_{cr}\}dxdy \tag{33}$$

where the first term is due to the bending of the generators given by Eq. (1) and the second term is due to the change $\varepsilon_0 - \varepsilon_{xm}$ of the axial strain. Assuming that during buckling the compressive load remains constant, then $N_x = N_{cr}$. Substituting Eqs. (1), (2), and (5) into Eq. (33), gives

$$W = \frac{A^2 m^2 \pi^3 R N_{cr}}{2L} - \frac{2\nu A L N_{cr}}{m}\{(-1)^m - 1\} \tag{34}$$

Equating expressions (32) and (34), results as

$$\frac{2C_1 \pi R L N_{cr}^{\ 2}}{h^2 E(z)^2} = 0 \tag{35}$$

$$\frac{4C_1 \nu L N_{cr}}{hmE(z)}\{(-1)^m - 1\} + \frac{2m\pi^2 R C_3 N_{cr}}{LhE(z)}\{(-1)^m - 1\} = \frac{-2\nu L N_{cr}}{m}\{(-1)^m - 1\} \tag{36}$$

$$\frac{C_5 m^4 \pi^5 R}{L^3(1-\nu^2)} + \frac{C_1 \pi L}{R} = \frac{m^2 \pi^3 R N_{cr}}{2L} \tag{37}$$

Relations (35) and (36) do not have any application, where using relation (37) gives

$$N_b = \frac{C_5 m^2 \pi^2}{L^2(1-\nu^2)} + \frac{C_1 L^2}{m^2 \pi^2 R^2} \tag{38}$$

In Eq. (38) N_{cr} is replaced by N_b (buckling load), because it is dependent to m. Assuming that there are many waves formed along the length of the cylinder during buckling and considering N_{cr} is the minimum value of N_b at a certain value of m, the minimum value of expression (38) occurs at

$$m = \frac{L}{\pi}\sqrt[4]{\frac{C_1(1-\nu^2)}{C_5 R^2}} \tag{39}$$

Substituting Eq. (39) in Eq. (38) for minimum value of N_b to give

$$N_{cr} = \frac{2}{R}\sqrt{\frac{C_1 C_5}{1-\nu^2}} \tag{40}$$

For pure isotropic cylinder $E(z) = cte$, and the value of C_1 and C_5 are Eh and $\frac{Eh^3}{12}$, respectively. Substituting these values in Eq. (40) gives

$$N_{cr} = \frac{Eh^2}{R\sqrt{3(1-\nu^2)}} \tag{41}$$

Relation (41) was first derived by Timoshenko [42].

This relationship can be extended for the inhomogeneous materials. Consider a thin cylindrical shell made of FGM. The shell is assumed to be graded through the thickness direction. The constituent materials are assumed to be ceramic and metal. The volume fractions of ceramic f_c and metal f_m corresponding to the power law are expressed as [43]

$$f_c = [(2z+h)/2h]^n, \qquad f_c = 1 - f_m \tag{42}$$

where z is the thickness coordinate, $-h/2 \le z \le h/2$, and n is the power law index, which takes values greater than or equal to zero. The value of n equal to zero represents a fully ceramic shell, and the value of n equal to infinite represents a fully metal shell. The mechanical and thermal properties of FGM are determined from the volume fraction of the material constituents. Assume that the inhomogeneous material properties such as the modulus of elasticity E change in the thickness direction z based on the Voigt's rule [43] over the whole range of volume fraction as [43]

$$E(z) = E_c f_c + E_m(1 - f_c) \tag{43}$$

$$\nu(z) = \nu \tag{44}$$

where subscripts m and c refer to the metal and ceramic constituents, respectively. When volume fractions are substituted from Eq. (42) in Eq. (43), the elastic modulus function for the shell made of FGM is determined, which is the same as the equation proposed by Praveen and Reddy [44] as

$$E(z) = E_m + E_{cm}\left(\frac{2z+h}{2h}\right)^n, \; E_{cm} = E_c - E_m \tag{45}$$

$$\nu(z) = \nu \tag{46}$$

Substituting Eq. (45) into Eq. (39), using the definitions for C_1 and C_5, gives

$$m = \frac{L}{\pi}\sqrt[4]{\frac{(1-\nu^2)(E_m + \frac{E_{cm}}{n+1})}{R^2\left(\frac{E_m}{12} + \frac{(n^2+n+2)E_{cm}}{4(n+1)(n+2)(n+3)}\right)}} \tag{47}$$

Relation (47) is defined when the outer surface of the shell is ceramic and the inner surface of the shell is metal. Substituting Eq. (45) into the relations defined for C_1 and C_5 and finally into Eq. (40) to give

$$N_{cr} = \frac{2h^2}{R\sqrt{1-\nu^2}}\left[\left(E_m + \frac{E_{cm}}{n+1}\right)\left(\frac{E_m}{12} + \frac{(n^2+n+2)E_{cm}}{4(n+1)(n+2)(n+3)}\right)\right]^{\frac{1}{2}} \tag{48}$$

Assuming that the outer surface of the shell is metal and the inner surface of the shell is ceramic, the elastic modulus varying model can be given as

$$E(z) = E_c + E_{mc}\left(\frac{2z+h}{2h}\right)^n, \; E_{mc} = E_m - E_c \tag{49}$$

Substituting Eq. (49) into Eq. (39), using the definitions for C_1 and C_5, gives

$$m=\frac{L}{\pi}\sqrt[4]{\frac{(1-\nu^2)(E_c+\frac{E_{mc}}{n+1})}{R^2(\frac{E_c}{12}+\frac{(n^2+n+2)E_{mc}}{4(n+1)(n+2)(n+3)})}} \tag{50}$$

and

$$N_{cr}=\frac{2h^2}{R\sqrt{1-\nu^2}}[(E_c+\frac{E_{mc}}{n+1})(\frac{E_c}{12}+\frac{(n^2+n+2)E_{mc}}{4(n+1)(n+2)(n+3)})]^{\frac{1}{2}} \tag{51}$$

Equations (48) and (51) for the value of n equal to zero reduce to relation (41) that was derived first by Timoshenko [42].

3 Example Analysis

As an example, consider a ceramic-metal functionally graded cylindrical shell. The combination of materials consists of steel and alumina. The Young modulus for steel is $E_m = 200\,\text{GPa}$ and for alumina is $E_c = 380\,\text{GPa}$, respectively. The Poisson ratio is assumed to be $\nu = 0.3$ for steel and alumina. Simply supported boundary conditions are assumed.

The variation of buckling load N_b verses the variation of buckling mode m is plotted for different values of power law index n in Figs. (3) and (4). These figures show the buckling load decreases with the increase of m. Figure (3) shows the buckling load decreases with the increase of n (the outer surface is ceramic and the inner surface is steel) and the highest buckling load is related to the pure ceramic ($n = 0$ in Eqs. (38) and (45)). Figure (4) shows that the buckling load increases with the increase of n (the outer surface is steel and the inner surface is ceramic) and the lowest buckling load is related to the pure steel ($n = 0$ in Eqs. (38) and (49)). In these figures $R = L = 1\text{m}$ and $h = 0.001\,\text{m}$ are considered.

The variation of critical buckling load N_{cr} versus the variation of shell thickness h is plotted for different values of the power law index n in Figs. (5) and (6). It is seen that the critical buckling load increases with the increase of h. Figure (5) shows that the critical buckling load decreases with the increase of n (the outer surface is ceramic and the inner surface is steel) and the highest critical buckling load is related to the pure ceramic ($n = 0$ in Eq. (48)). Figure (6) shows that the critical buckling load increases with the increase of n (the outer surface is steel and the inner surface is ceramic) and the lowest critical buckling load is related to the pure steel ($n = 0$ in Eq. (51)). In these figures $R = 1\text{m}$ is considered.

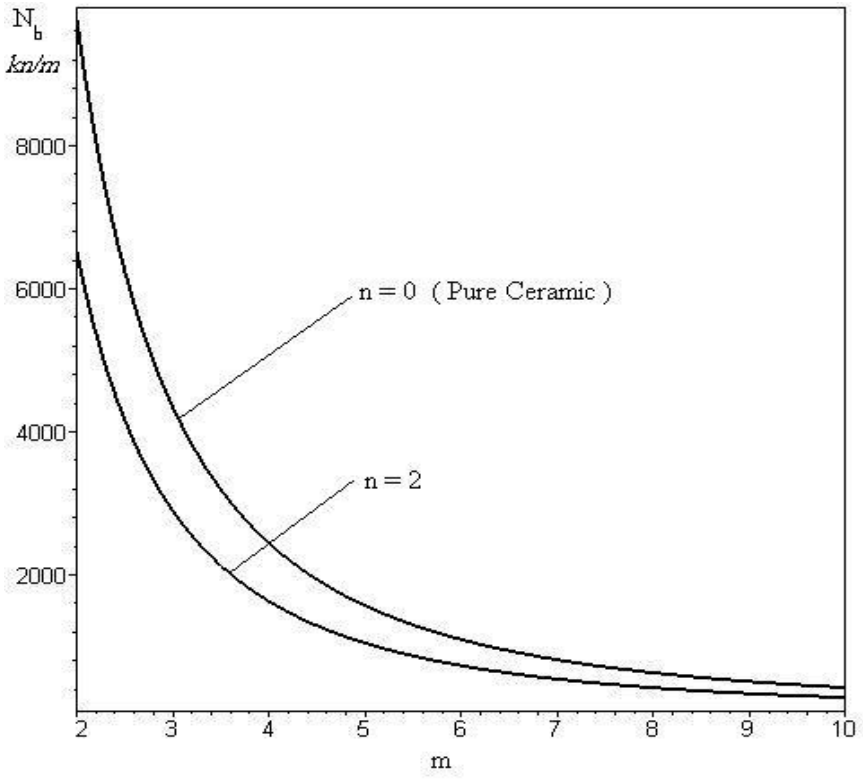

Figure 3 Variation of the Buckling Load vs m and for Various Values of n
(the outer surface is ceramic and the inner surface is steel and $R = 1\text{m}$, $h = 0.001\,\text{m}$, and $L = R$)

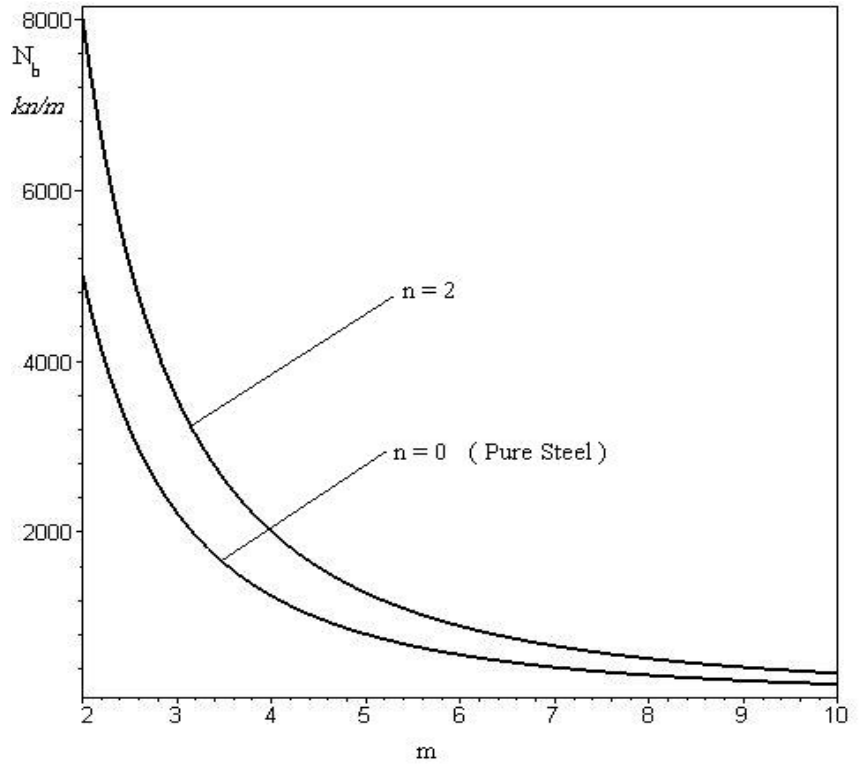

Figure 4 Variation of the Buckling Load vs m and for Various Values of n
(the outer surface is steel and the inner surface is ceramic and $R = 1\text{m}$, $h = 0.001\,\text{m}$,, and $L = R$)

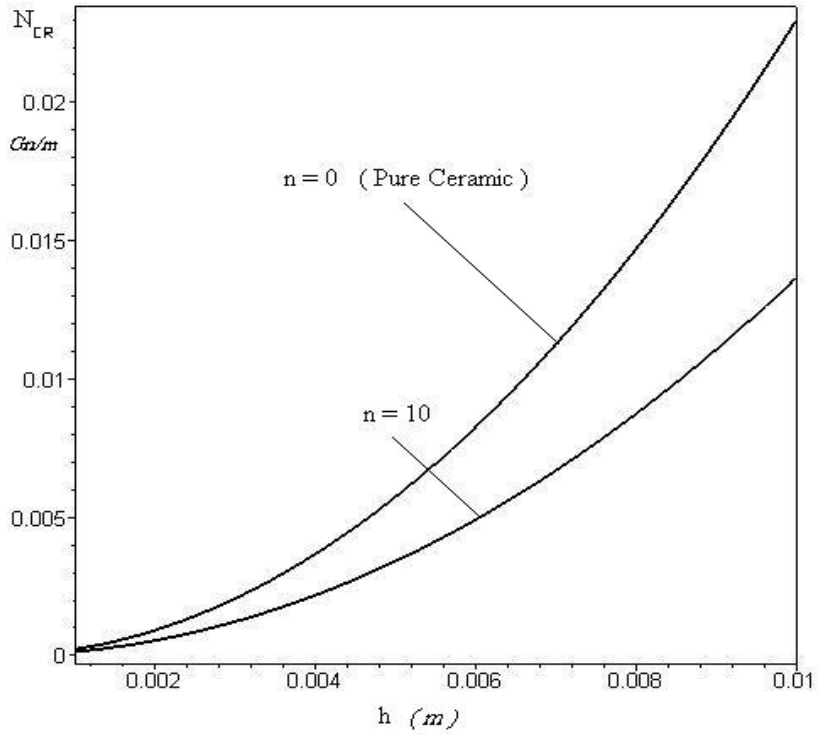

Figure 5 Variation of the Critical Buckling Load vs h and for Various Values of n (the outer surface is ceramic and the inner surface is steel and $R = 1\text{m}$)

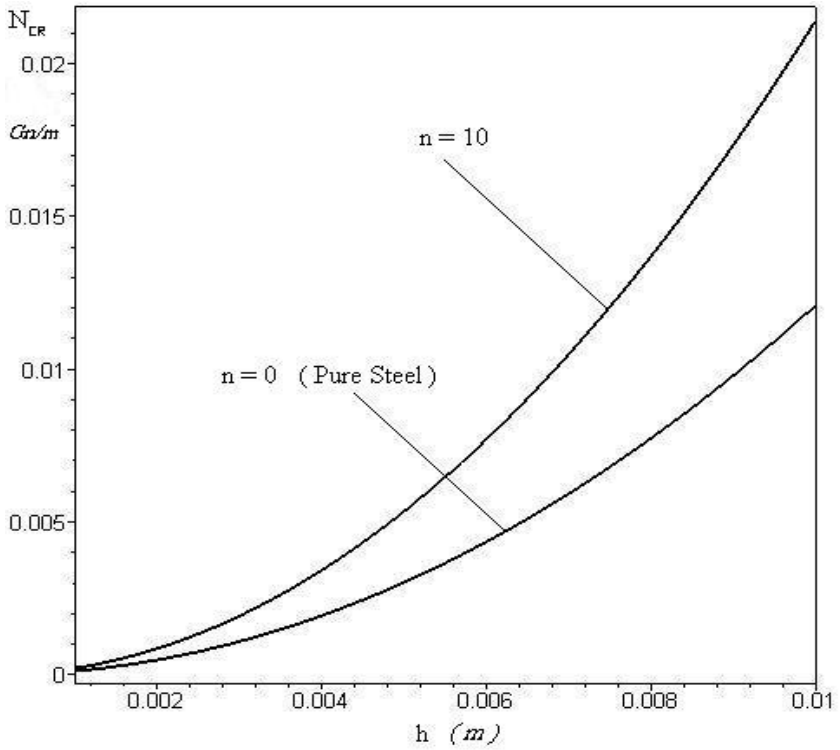

Figure 6 Variation of the Critical Buckling Load vs h and for Various Values of n (the outer surface is steel and the inner surface is ceramic and $R = 1\text{m}$)

The variation of buckling load N_b versus the variation of length of the shell L is plotted for different values of the power law index n and the buckling mode $m = 10$ in Figs. (7) and (8). These figures show the buckling load increases with the increase of L ???????????. Figure (7) shows that the buckling load decreases with the increase of n (the outer surface is ceramic and the inner surface is steel) and the highest buckling load is related to the pure ceramic ($n = 0$ in Eq. (48)). Figure (8) shows the buckling load increases with the increase of n (the outer surface is steel and the inner surface is ceramic) and the lowest buckling load is related to the pure steel ($n = 0$ in Eq. (51)). In these figures $R = 1\,\text{m}$ and $h = 0.001\,\text{m}$ are considered.

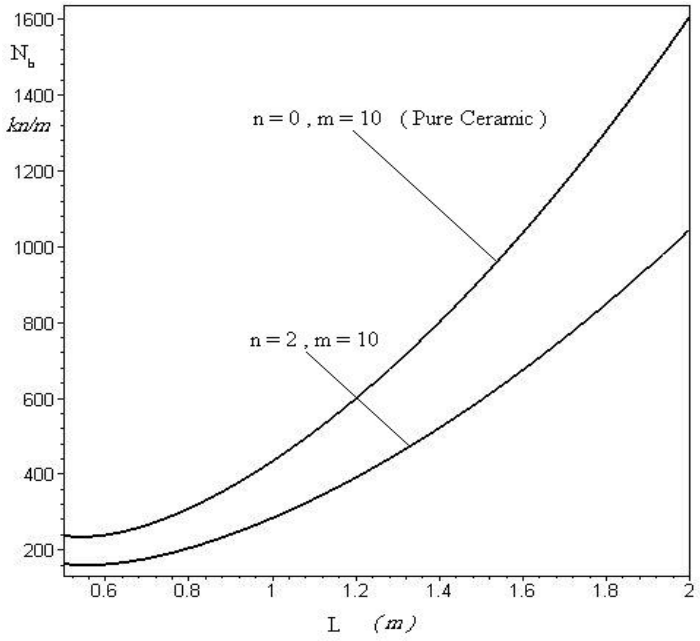

Figure 7 Variation of the Buckling Load vs L and for Various Values of n
(the outer surface is ceramic and the inner surface is steel and $R = 1\,\text{m}$, $h = 0.001\,\text{m}$)

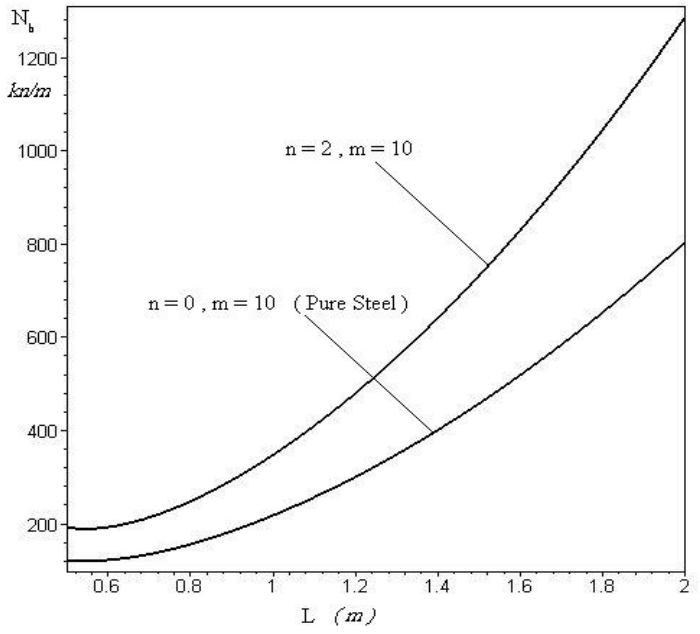

Figure 8 Variation of the Buckling Load vs L and for Various Values of n
(the outer surface is steel and the inner surface is ceramic and $R = 1\,\text{m}$, $h = 0.001\,\text{m}$)

4 Conclusions

In this article, the axisymmetric critical buckling load of cylindrical shells made of FGM under uniform axial compressive load is obtained and compared with an earlier buckling formula given by Timoshenko [42]. Derivations are based on the first-order shell theory, the Sanders simplified kinematic relations, the principle of work and energy, and Timoshenko's assumptions [42]. The following conclusions are reached:

1) The buckling load N_b for cylindrical shell made of FGM is function of the length of the shell L.
2) The critical buckling load N_{cr} for cylindrical shell made of FGM is not function of the length of the shell L.
3) The buckling load N_b and the critical buckling load N_{cr} for cylindrical shell made of FGM are function of the coefficients C_1 and C_5.
4) The buckling load N_b for cylindrical shell made of FGM decreases with the increase of the buckling mode m and mean radius R and increases with the increase of length of the shell L and shell thickness h.
5) The buckling load N_b and the critical buckling load N_{cr} for cylindrical shell made of FGM are smaller or greater than the corresponding values for the pure isotropic cylindrical shell. It is strongly dependent to the defined mechanical properties function.
6) The closed form solution presented in this article can be used for analyse of different FGM properties with varying gradients. In the extreme case of barrier coatings the method can model also the sharp gradient at the metal–ceramic interface.
7) The bending and stretching strain energy equations for cylindrical shell made of FGM are not identical with the corresponding equations for the pure isotropic cylindrical shell expressed in the form of forces, strains, and curvatures.
8) The buckling mode m associated with minimum buckling load N_b for cylindrical shell made of FGM increases with the increase of L and C_1 and decreases with the increase of ν, C_5, and R.

References

[1] Eslami, M. R., Ziaii, A. R., and Ghorbanpour, A., “Thermoelastic Buckling of Thin Cylindrical Shells Based on Improved Donnell Equations”, J. Thermal Stresses, Vol. 19, pp. 299-316, (1990).

[2] Eslami, M. R., and Javaheri, R., “Thermal and Mechanical Buckling of Composite Cylindrical Shells”, J. Thermal Stresses, Vol. 22, No. 6, pp. 527-545, (1999).

[3] Eslami, M. R., and Shariyat, M., “A High-order Theory for Dynamic Buckling and Post Buckling Analysis of Laminated Cylindrical Shell”, J. ASME, Pressure Vessel Tech., Vol. 121, pp. 94-102, (1999).

[4] Eslami, M. R., and Shariyat, M., “Dynamic Buckling and Post Buckling of Imperfect Orthotropic Cylindrical Shells under Mechanical and Thermal Loads Based on the Three-dimensional Theory of Elasticity”, J. ASME, Appl. Mech., Vol. 66, pp. 476-484, (1999).

[5] Eslami, M. R., and Shariyat, M., "Elastic, Plastic, and Creep Buckling of Imperfect Cylinders under Mechanical and Thermal Loading", J. ASME, Pressure Vessel Tech., Vol. 118, No. 1, pp. 27-36, (1997).

[6] Eslami, M. R., and Shahsiah, R., "Thermal Buckling of Imperfect Cylindrical Shells", J. Thermal Stresses, Vol. 24, No. 1, pp. 71-90, (2000).

[7] Birman, V., and Bert, C. W., "Buckling and Post Buckling of Composite Plates and Shells Subjected to Elevated Temperature", Trans. ASME, J. Appl. Mech., Vol. 60, pp. 514-519, (1993).

[8] Shen, H. S., "Post Buckling Analysis of Imperfect Stiffened Laminated Cylindrical Shells under Combined External Pressure and Axial Compression", J. Computers and Structures, Vol. 63, pp. 335-348, (1997).

[9] Shen, H. S., "Post Buckling Analysis of Imperfect Stiffened Laminated Cylindrical Shells under Combined External Pressure and Thermal Loading", Int. J. Mechanical Sciences, Vol. 40, pp. 339-355, (1998).

[10] Shen, H. S., "Thermo-mechanical Post Buckling of Composite Laminated Cylindrical Shells with Local Geometric Imperfections", Int. J. Solids and Structures, Vol. 36, pp. 597-617, (1999).

[11] Iu, V. P., and Chia, C. Y., "Effect of Transverse Shear on Nonlinear Vibration and Post Buckling of Anti Symmetric Cross Ply Imperfect Cylindrical Shells", Int. J. Mechanical Sciences, Vol. 30, pp. 705-718, (1988).

[12] Reddy, J. N., and Savoia, M., "Layer-wise Shell Theory for Post Buckling of Laminated Circular Cylindrical Shells", J. AIAA, Vol. 30, pp. 2148-2154, (1992).

[13] Whitney, J. M., and Ashton, J. E., "Effect of Environment on the Elastic Response of Layered Composite Plates", J. AIAA, Vol. 9, pp. 1708-1713, (1971).

[14] Snead, J. M., and Palazotto, A. N., "Moisture and Temperature Effects on the Instability of Cylindrical Composite Panels", J. Aircraft, Vol. 20, pp. 777-783, (1983).

[15] Lee, S. Y., and Yen, W. J., "Hygrothermal Effects on the Stability of a Cylindrical Composite Shell Panel, J. Computers and Structures", Vol. 33, pp. 551-559, (1989).

[16] Ram, K. S. S., and Sinha, P. K., "Hygrothermal Effects on the Buckling of Laminated Composite Structures", Vol. 21, pp. 233-247, (1992).

[17] Chao, L. P., and Shyu, S. L., "Nonlinear Buckling of Fiber Reinforced Composite Plates under Hygrothermal Effects", J. Chinese Institute of Engineers, Vol. 19, pp. 657-667, (1996).

[18] Palazotto, A. N., and Tisler, T. W., "Experimental Collapse Determination of Cylindrical Composite Panels with Large Cutouts under Axial Load", J. Composite Structures, Vol. 12, pp. 61-78, (1989).

[19] Palazotto, A. N., “An Experimental Study of a Curved Composite Panel with a Cutout, J. American Society for Testing and Materials”, Vol. 972, pp. 191-202, (1988).

[20] Horban, B. A., and Palazotto, A. N., “Experimental Buckling of Cylindrical Composite Panels with Eccentrically Located Circular Delaminations”, J. Spacecraft and Rockets, Vol. 24, pp. 349-352, (1987).

[21] Siefert, G. R., and Palazotto, A. N., “The Effect of a Centrally Located Midplane Delamination on the Stability of Composite Panels”, J. Experimental Mechanics, Vol. 26, pp. 330-336, (1986).

[22] Dennis, S. T., and Palazotto, A. N., “Large Displacement and Rotational Formulation for Laminated Shells Including Parabolic Transverse Shear”, Int. J. Nonlinear Mechanics, Vol. 25, pp. 67-85, (1990).

[23] Dennis, S. T., and Palazotto, A. N., “Transverse Shear Deformation in Orthotropic Cylindrical Pressure Vessels using a High-order Shear Theory”, J. AIAA, Vol. 27, pp. 1441-1447, (1989).

[24] Tsai, C. T., Palazotto, A. N., and Dennis, S. T., “Large Rotation Snap Through Buckling in Laminated Cylindrical Panels”, J. Finite Elements in Analysis and Design, Vol. 9, pp. 65-75, (1991).

[25] Dennis, S. T., and Palazotto, A. N., “Effect of Nonlinear Curvature Strains on the Buckling of Laminated Plates and Shells”, Int. J. Numerical Methods in Engineering, Vol. 36, pp. 595-610, (1993).

[26] Schimmels, S. A., and Palazotto, A. N., “Nonlinear Geometric and Material Behavior of Composite Shells with Large Strains”, J. Engineering Mechanics, Vol. 120, pp. 320-345, (1994).

[27] Palazotto, A. N., Chien, L. S., and Taylor, W. W., “Stability Characteristics of Laminated Cylindrical Panels under Transverse Loading”, J. AIAA, Vol. 30, pp. 1649-1653, (1992).

[28] Chien, L. S., and Palazotto, A. N., “Dynamic Buckling of Composite Cylindrical Panels with Higher-order Transverse Shear Subjected to a Transverse Concentrated Load”, Int. J. Nonlinear Mechanics, Vol. 27, pp. 719-734, (1992).

[29] Schimmels, S. A., and Palazotto, A. N., “Collapse Characteristics of Cylindrical Panels under Axial Loads”, J. AIAA, Vol. 30, pp. 1447-1466, (1992).

[30] Shen, H. S., “Hygrothermal Effects on the Post Buckling of Composite Laminated Cylindrical Shells”, J. Composite Science and Technology, Vol. 60, pp. 1227-1240, (2000).

[31] Birman, V., “Buckling of Functionally Graded Hybrid Composite Plates”, Proceeding of the 10th Conference on Engineering Mechanics, Vol. 2, pp. 1199-1202, New York, USA, (1995).

[32] Ng, T. Y., Lam, Y. K., Liew, K. M., and Reddy, J. N., "Dynamic Stability Analysis of Functionally Graded Cylindrical Shell under Periodic Axial Loading", Int. J. Solids and Structures, Vol. 38, pp. 1295-1300, (2001).

[33] Shahsiah, R., and Eslami, M. R., "Thermal Buckling of Functionally Graded Cylidrical Shell", J. Thermal Stresses,Vol. 26, No. 3, pp. 277-294, (2003).

[34] Shahsiah, R., and Eslami, M. R., "Functionally Graded Cylindrical Shell Thermal Instability Based on Improved Donnell Equations", J. AIAA, Vol. 41, No. 9, pp. 1819-1826, (2003).

[35] Shahsiah, R., Eslami, M. R., and Naj, R., "Thermal Instability of Functionally Graded Shallow Spherical Shell", J. Thermal Stresses, Vol. 29, No. 8, pp. 771-790, (2006).

[36] Najafizadeh, M. M., and Eslami, M. R., "First Order Theory Based Thermoelastic Stability of Functionally Graded Material Circular Plates", J. AIAA, Vol. 40, No. 7, pp. 444-450, (2002).

[37] Javaheri, R., and Eslami, M. R., "Thermoelastic Buckling of Rectangular Plates Made of Functionally Graded Materials", J. AIAA, Vol. 40, No. 1, pp. 162-169, (2002).

[38] Javaheri, R., and Eslami, M. R., "Buckling of Functionally Graded Plates under In-Plane Compressive Loading", ZAMM, Vol. 82, No. 4, pp. 277-283, (2002).

[39] Javaheri, R., and Eslami, M. R., "Buckling of Functionally Graded Plates under In-plane Compressive Loading Based on Various Plate Theories", J. Iranian Society of Mechanical Engineers, Vol. 6, No. 1, pp. 76-93, (2005).

[40] Javaheri, R., and Eslami, M. R., "Thermal Buckling of Functionally Graded Plates Based on Higher Order Theory", J. Thermal Stresses, Vol. 25, No. 7, pp. 603-625, (2002).

[41] Brush, D. O., and Almroth, B. O., "*Buckling of Bars, Plates and Shells*", McGraw-Hill, New York, (1975).

[42] Timoshenko, S. P., and Gere, J. M., "*Theory of Elastic Stability*", McGraw-Hill, New York, (1960).

[43] Suresh, S., and Mortensen, A., "*Fundamentals of Functionally Graded Materials*", Cambridge Uni. Press, London, (1998).

[44] Praveen, G. N., and Reddy, J. N., "Nonlinear Transient Thermoelastic Analysis of Functionally Graded Ceramic Metal Plates", Int. J. Solids and Structures, Vol. 35, No. 33, pp. 4457-4476, (1998).

Nomenclature

D : bending stiffness
E_m, E_c : elastic modulus of metal and ceramic
$E(z)$: elastic modulus varying continuous function of FGM
$G(z)$: shear modulus varying continuous function of FGM
ν : Poisson's ratio
f_m, f_c : volume fraction of metal and ceramic
h : thickness of functionally graded cylindrical shell
L : length of functionally graded cylindrical shell
R : mean radius of functionally graded cylindrical shell
k_{ij} : curvatures of middle surface
M_{ij} : moment resultants
N_{ij} : force resultants
N_b : buckling load
N_{cr} : critical buckling load
σ_i : normal stresses
τ_{ij} : shear stress
m : number of longitudinal buckling waves (buckling modes)
n : power index in mechanical properties varying models
U_b : strain energy due to bending
U_s : strain energy due to stretching
W : work done during buckling
v : circumferential displacement
w : lateral displacement
ε_{ij} : shear strain at distance z from the shell middle surface
ε_{ijm} : shear strain of middle surface
ε_i : normal strains at distance z from the shell middle surface
ε_{im} : normal strains of middle surface
ε_0 : prebuckling normal strain

Appendix (1)

$$C_1 = \int_{-h/2}^{h/2} E(z)dz$$

$$C_2 = \int_{-h/2}^{h/2} G(z)dz$$

$$C_3 = \int_{-h/2}^{h/2} zE(z)dz$$

$$C_4 = 2\int_{-h/2}^{h/2} zG(z)dz$$

$$C_5 = \int_{-h/2}^{h/2} z^2 E(z)dz$$

$$C_6 = 2\int_{-h/2}^{h/2} z^2 G(z)dz$$

Appendix (2)

$$U = \iiint_{\forall} \frac{1}{2}\frac{E(z)}{1-\nu^2}(\varepsilon_{xm}{}^2 + \varepsilon_{\theta m}{}^2 + z^2 k_x{}^2 + z^2 k_\theta{}^2 - 2z\varepsilon_{xm}k_x - 2z\varepsilon_{\theta m}k_\theta + 2\nu\varepsilon_{xm}\varepsilon_{\theta m}$$

$$-2\nu z\varepsilon_{xm}k_\theta - 2\nu z\varepsilon_{\theta m}k_x + 2\nu z^2 k_x k_\theta + \frac{1-\nu}{2}\varepsilon_{x\theta m}{}^2 + 2(1-\nu)z^2 k_{x\theta}{}^2$$

$$-2(1-\nu)z\varepsilon_{x\theta m}k_{x\theta})d\forall = \frac{1}{2}\iiint_{\forall}\frac{E(z)}{1-\nu^2}[\varepsilon_{xm}(\varepsilon_{xm} - 2zk_x + \nu\varepsilon_{\theta m} - 2z\nu k_\theta) + \varepsilon_{\theta m}(\varepsilon_{\theta m}$$

$$-2zk_\theta + \nu\varepsilon_{xm} - 2z\nu k_x) + \frac{1-\nu}{2}\varepsilon_{x\theta m}(\varepsilon_{x\theta m} - 4zk_{x\theta}) + z^2(k_x{}^2 + k_\theta{}^2 + 2\nu k_x k_\theta +$$

$$2(1-\nu)k_{x\theta}{}^2)]d\forall = \frac{1}{2}\iiint_{\forall}\frac{E(z)}{1-\nu^2}[\varepsilon_{xm}(\varepsilon_{xm} + \nu\varepsilon_{\theta m} - z\{k_x + \nu k_\theta\}) - z\varepsilon_{xm}(k_x + \nu k_\theta) +$$

$$\varepsilon_{\theta m}(\varepsilon_{\theta m} + \nu\varepsilon_{xm} - z\{k_\theta + \nu k_x\}) - z\varepsilon_{\theta m}(k_\theta + \nu k_x) + \frac{1-\nu}{2}\varepsilon_{x\theta m}(\varepsilon_{x\theta m} - 2zk_{x\theta}) -$$

$$z(1-\nu)k_{x\theta}\varepsilon_{x\theta m} + z^2(k_x{}^2 + k_\theta{}^2 + 2\nu k_x k_\theta + 2(1-\nu)k_{x\theta}{}^2)]d\forall = \frac{1}{2}\int_x\int_\theta\{\varepsilon_{xm}\int_{-h/2}^{h/2}[\frac{E(z)}{1-\nu^2}($$

$$\varepsilon_{xm} + \nu\varepsilon_{\theta m} - z(k_x + \nu k_\theta))]dz + \varepsilon_{\theta m}\int_{-h/2}^{h/2}[\frac{E(z)}{1-\nu^2}(\varepsilon_{\theta m} + \nu\varepsilon_{xm} - z(k_\theta + \nu k_x))]dz$$

$$-\int_{-h/2}^{h/2}[z\frac{E(z)}{1-\nu^2}\varepsilon_{xm}(k_x + \nu k_\theta) - z\frac{E(z)}{1-\nu^2}\varepsilon_{\theta m}(k_\theta + \nu k_x)]dz + \varepsilon_{x\theta m}\int_{-h/2}^{h/2}[\frac{E(z)}{2(1+\nu)}(\varepsilon_{x\theta m}$$

$$-2zk_{x\theta})]dz + (k_x{}^2 + k_\theta{}^2 + 2\nu k_x k_\theta + 2(1-\nu)k_{x\theta}{}^2)\int_{-h/2}^{h/2}\frac{z^2 E(z)}{1-\nu^2}dz\}dxd\theta$$

$$U = \frac{1}{2}\int_x\int_\theta(N_x\varepsilon_{xm} + N_\theta\varepsilon_{\theta m} - \frac{C_3}{1-\nu^2}\varepsilon_{xm}(k_x + \nu k_\theta) - \frac{C_3}{1-\nu^2}\varepsilon_{\theta m}(k_\theta + \nu k_x)$$

$$+ N_{x\theta}\varepsilon_{x\theta m})dxd\theta + \frac{1}{2}\frac{C_5}{1-\nu^2}\int_x\int_\theta[k_x{}^2 + k_\theta{}^2 + 2\nu k_x k_\theta + 2(1-\nu)k_{x\theta}{}^2]dxd\theta$$

Appendix (3)

$$U = \frac{C_5}{2(1-\nu^2)}\int_A[w,_{xx}{}^2 + \frac{1}{R^4}(v,_\theta{}^2 + w,_{\theta\theta}{}^2 + 2v,_\theta w,_{\theta\theta}) + \frac{2\nu}{R^2}v,_\theta w,_{xx} + \frac{2\nu}{R^2}w,_{xx}w,_{\theta\theta} +$$

$$\frac{2(1-\nu)}{R^2}(v,_x{}^2 + w,_{x\theta}{}^2 + 2v,_x w,_{x\theta})]dA + \frac{1}{2}\int_A[\frac{C_1}{1-\nu^2}(\varepsilon_0{}^2 + \frac{\nu^2 w^2}{R^2} + \frac{2\varepsilon_0\nu w}{R} - \nu^2\varepsilon_0{}^2 -$$

$$\frac{\nu^3\varepsilon_0 w}{R} - \frac{\nu\varepsilon_0 w}{R} - \frac{\nu^2 w^2}{R^2}) - \frac{C_3}{1-\nu^2}(w,_{xx}\varepsilon_0 + \frac{\nu w w,_{xx}}{R} + \frac{\nu\varepsilon_0 v,_\theta}{R^2} + \frac{\nu^2 w v,_\theta}{R^3} + \frac{\nu\varepsilon_0 w,_{\theta\theta}}{R^2} +$$

$$\frac{\nu^2 ww_{,\theta\theta}}{R^3}) + \frac{C_1}{1-\nu^2}(\nu^2 {\varepsilon_0}^2 + \frac{w^2}{R^2} + \frac{2\nu\varepsilon_0 w}{R} - \nu^2 {\varepsilon_0}^2 - \frac{\nu^3\varepsilon_0 w}{R} - \frac{\nu\varepsilon_0 w}{R}$$
$$- \frac{\nu^2 w^2}{R^2}) + \frac{C_3}{1-\nu^2}(\frac{\nu\varepsilon_0 v_{,\theta}}{R^2} + \frac{\nu\varepsilon_0 w_{,\theta\theta}}{R^2} + \frac{wv_{,\theta}}{R^3} + \frac{ww_{,\theta\theta}}{R^3} + \nu^2\varepsilon_0 w_{,xx} + \nu\frac{ww_{,xx}}{R})$$
$$+ C_2 {\varepsilon_{x\theta m}}^2 - \frac{C_4\varepsilon_{x\theta m}}{R}(v_{,x} + w_{,x\theta}) - \frac{C_3}{1-\nu^2}(\varepsilon_0 w_{,xx} + \frac{\nu ww_{,xx}}{R} + \frac{\nu\varepsilon_0 v_{,\theta}}{R^2} + \frac{\nu\varepsilon_0 w_{,\theta\theta}}{R^2}$$
$$+ \frac{\nu^2 wv_{,\theta}}{R^3} + \frac{\nu^2 ww_{,\theta\theta}}{R^3} - \frac{\nu\varepsilon_0 v_{,\theta}}{R^2} - \frac{\nu\varepsilon_0 w_{,\theta\theta}}{R^2} - \frac{wv_{,\theta}}{R^3} - \frac{ww_{,\theta\theta}}{R^3} - \nu^2\varepsilon_0 w_{,xx} - \frac{\nu ww_{,xx}}{R})]dA$$

Appendix (4)

$$\Delta U = \frac{C_5}{2(1-\nu^2)}\int_A [2w_{,xx}\Delta w_{,xx} + \frac{1}{R^4}(2v_{,\theta}\Delta v_{,\theta} + 2w_{,\theta\theta}\Delta w_{,\theta\theta} + 2\Delta v_{,\theta} w_{,\theta\theta}$$
$$+ 2v_{,\theta}\Delta w_{,\theta\theta}) + \frac{2\nu}{R^2}\Delta v_{,\theta} w_{,xx} + \frac{2\nu}{R^2} v_{,\theta}\Delta w_{,xx} + \frac{2\nu}{R^2}\Delta w_{,xx} w_{,\theta\theta} +$$
$$\frac{2\nu}{R^2} w_{,xx}\Delta w_{,\theta\theta} + \frac{4(1-\nu)}{R^2} v_{,x}\Delta v_{,x} + \frac{4(1-\nu)}{R^2} w_{,x\theta}\Delta w_{,x\theta} + \frac{4(1-\nu)}{R^2} \times$$
$$\Delta v_{,x} w_{,x\theta} + \frac{4(1-\nu)}{R^2} v_{,x}\Delta w_{,x\theta}]dA + \frac{1}{2}\int_A [\frac{2C_1\varepsilon_0\Delta\varepsilon_0}{1-\nu^2} + \frac{2\nu^2 C_1 w\Delta w}{R^2(1-\nu^2)} +$$
$$\frac{2\varepsilon_0 C_1\nu\Delta w + 2\nu C_1 w\Delta\varepsilon_0}{R(1-\nu^2)} - \frac{2\nu^2 C_1\varepsilon_0\Delta\varepsilon_0}{1-\nu^2} - \frac{C_1\nu^3\Delta\varepsilon_0 w + C_1\nu^3\varepsilon_0\Delta w}{R(1-\nu^2)} -$$
$$\frac{C_1\nu\Delta\varepsilon_0 w + C_1\nu\varepsilon_0\Delta w}{R(1-\nu^2)} - \frac{2C_1\nu^2 w\Delta w}{R^2(1-\nu^2)} - \frac{C_3\Delta w_{,xx}\varepsilon_0 + C_3 w_{,xx}\Delta\varepsilon_0}{1-\nu^2}$$
$$+ \frac{C_3\nu\Delta\varepsilon_0 v_{,\theta} + C_3\nu\varepsilon_0\Delta v_{,\theta}}{R^2(1-\nu^2)} + \frac{C_3\nu\Delta\varepsilon_0 w_{,\theta\theta} + C_3\nu\varepsilon_0\Delta w_{,\theta\theta}}{R^2(1-\nu^2)} + \frac{C_3\Delta wv_{,\theta} + C_3 w\Delta v_{,\theta}}{R^3(1-\nu^2)} +$$
$$\frac{C_3\Delta ww_{,\theta\theta} + C_3 w\Delta w_{,\theta\theta}}{R^3(1-\nu^2)} + \frac{C_3\nu^2\Delta\varepsilon_0 w_{,xx} + C_3\nu^2\varepsilon_0\Delta w_{,xx}}{1-\nu^2} + \frac{C_3\nu\Delta ww_{,xx} + C_3\nu w\Delta w_{,xx}}{R(1-\nu^2)}$$
$$- \frac{C_3\nu\Delta w w_{,xx} + C_3\nu w\Delta w_{,xx}}{R(1-\nu^2)} - \frac{C_3\nu\Delta\varepsilon_0 v_{,\theta} + C_3\nu\varepsilon_0\Delta v_{,\theta}}{R^2(1-\nu^2)} - \frac{\nu^2 C_3}{R^3(1-\nu^2)}\Delta w v_{,\theta}$$

$$-\frac{\nu^2 C_3 w\Delta v_{,\theta}}{R^3(1-\nu^2)}-\frac{C_3\nu\Delta\varepsilon_0 w_{,\theta\theta}+C_3\nu\varepsilon_0\Delta w_{,\theta\theta}}{R^2(1-\nu^2)}-\frac{C_3\nu^2\Delta w w_{,\theta\theta}+C_3\nu^2 w\Delta w_{,\theta\theta}}{R^3(1-\nu^2)}+$$

$$\frac{2C_1\nu^2\varepsilon_0\Delta\varepsilon_0}{1-\nu^2}+\frac{2C_1 w\Delta w}{R^2(1-\nu^2)}+\frac{2\nu C_1\Delta\varepsilon_0 w+2\nu C_1\varepsilon_0\Delta w}{R(1-\nu^2)}-\frac{2C_1\nu^2\varepsilon_0\Delta\varepsilon_0}{1-\nu^2}-$$

$$\frac{\nu^3 C_1}{R(1-\nu^2)}\Delta\varepsilon_0 w-\frac{\nu^3 C_1\varepsilon_0\Delta w}{R(1-\nu^2)}-\frac{\nu C_1\Delta\varepsilon_0 w}{R(1-\nu^2)}-\frac{\nu C_1\varepsilon_0\Delta w}{R(1-\nu^2)}-\frac{2C_1\nu^2 w\Delta w}{R^2(1-\nu^2)}+$$

$$\frac{C_3\nu\Delta\varepsilon_0 v_{,\theta}+C_3\nu\varepsilon_0\Delta v_{,\theta}}{R^2(1-\nu^2)}+\frac{C_3\nu\Delta\varepsilon_0 w_{,\theta\theta}+C_3\nu\varepsilon_0\Delta w_{,\theta\theta}}{R^2(1-\nu^2)}+\frac{C_3\Delta w v_{,\theta}+C_3 w\Delta v_{,\theta}}{R^3(1-\nu^2)}+$$

$$\frac{C_3\Delta w w_{,\theta\theta}+C_3 w\Delta w_{,\theta\theta}}{R^3(1-\nu^2)}+\frac{C_3\nu^2\Delta\varepsilon_0 w_{,xx}+C_3\nu^2\varepsilon_0\Delta w_{,xx}}{1-\nu^2}+\frac{C_3\nu\Delta w w_{,xx}+C_3\nu w\Delta w_{,xx}}{R(1-\nu^2)}$$

$$+2C_2\varepsilon_{x\theta m}\Delta\varepsilon_{x\theta m}-\frac{C_4\Delta\varepsilon_{x\theta m}v_{,x}+C_4\varepsilon_{x\theta m}\Delta v_{,x}}{R}-\frac{C_4\Delta\varepsilon_{x\theta m}w_{,x\theta}+C_4\varepsilon_{x\theta m}\Delta w_{,x\theta}}{R}-\frac{C_3}{1-\nu^2}$$

$$\Delta\varepsilon_0 w_{,xx}-\frac{C_3}{1-\nu^2}\varepsilon_0\Delta w_{,xx}-\frac{C_3\nu\Delta w w_{,xx}+C_3\nu w\Delta w_{,xx}}{R(1-\nu^2)}-\frac{\nu C_3\Delta\varepsilon_0 v_{,\theta}+\nu C_3\varepsilon_0\Delta v_{,\theta}}{R^2(1-\nu^2)}-$$

$$\frac{C_3\nu\Delta\varepsilon_0 w_{,\theta\theta}+C_3\nu\varepsilon_0\Delta w_{,\theta\theta}}{R^2(1-\nu^2)}-\frac{C_3\nu^2\Delta w v_{,\theta}+C_3\nu^2 w\Delta v_{,\theta}}{R^3(1-\nu^2)}-\frac{C_3\nu^2\Delta w w_{,\theta\theta}+C_3\nu^2 w\Delta w_{,\theta\theta}}{R^3(1-\nu^2)}]dA$$

چکیده

در این مقاله، کمانش مکانیکی متقارن محوری، پوسته استوانه‌ای جدار نازک که از مواد مدرج تابعی ساخته شده، مورد بررسی قرار گرفته است. با در نظر گرفتن نظریه پوسته مرتبه اول و فرضیات تیموشنکو، معادلات حاکم بر استوانه جدار نازک بدست آمده‌اند. با استفاده از اصل کار و انرژی و روابط ساده شده سندرز برای تغییر شکل هندسی، معادلات تعادل و پایداری استخراج شده‌اند. ساختار ماده مدرج تابعی، مخلوطی از سرامیک به عنوان نافلز و فولاد به عنوان فلز در نظر گرفته شده است. فرض شده، خواص مکانیکی در ضخامت به شکل پیوسته تغییر نمایند. استوانه جدارنازک، تحت بار فشاری محوری که یکنواخت می باشد قرار دارد. در پایان، رابطه‌ای صریح برای بار کمانش مکانیکی بحرانی با روش تحلیلی ارائه شده است. نتایج با رابطه بدست آمده توسط تیموشنکو که در نوشتجات موجود است، اعتبار سنجی شده است.